Thin Solid Films 518 (2010) 5813–5819

Contents lists available at ScienceDirect

Thin Solid Films

journal homepage: www.elsevier.com/locate/tsf

Influence of Ru/Ru–SiO_2 underlayers on the microstructure and magnetic properties of CoPt–SiO_2 perpendicular recording media

Rujun Tang [a,b,*], Pin Ho [b], Boon Chow Lim [c]

[a] State key Laboratory of Electronic Thin Films and Integrated Devices, University of Electronic Science and Technology of China, Chengdu, 610054, China
[b] Department of Materials Science and Engineering, National University of Singapore, 117576, Singapore
[c] Data Storage Institute, (A*STAR) Agency for Science, Technology and Research, DSI Building, 5 Engineering Drive 1, 117608, Singapore

ARTICLE INFO

Available online 24 May 2010

Keywords:
CoPt recording media
Ru underlayer
Silicon dioxide volume fraction
Deposition pressure
Microstructure
Magnetic properties

ABSTRACT

SiO_2 was doped into Ru underlayer to reduce the grain size of CoPt–SiO_2 perpendicular media. The effects of SiO_2 volume fraction and sputtering deposition pressure of Ru–SiO_2 underlayer on the microstructure and magnetic properties of CoPt–SiO_2 media were studied. Increasing SiO_2 volume fraction in Ru–SiO_2 layer decreased the grain sizes of Ru and CoPt. Adding 5% SiO_2 to Ru–SiO_2 layer increased the coercivity and enhanced the exchange decoupling and thermal stability of CoPt–SiO_2 layer. A further increase in SiO_2 volume fraction caused the deterioration of magnetic properties of CoPt–SiO_2 layer. Deposition of Ru–SiO_2 layer at 1.3 Pa resulted in a smaller activation volume and higher thermal stability of the CoPt–SiO_2 media than that deposited at 0.4 Pa.

1. Introduction

One of the major challenges in further increasing the areal density of perpendicular magnetic recording media is in reducing the grain size and improving the signal to noise ratio by minimizing transition noise [1]. Efforts have been made to reduce grain size by adding oxide-based materials into the magnetic layer [2] or by depositing the magnetic layer in an argon and oxygen environment [3]. However, too much oxide in the magnetic layer would reduce its magnetic anisotropy, leading to increased thermal instability due to the superparamagnetic effect. An alternative approach is to reduce the grain size of the intermediate layer and hence, the grain size of the magnetic layer. The addition of synthetic nucleation layers [4], RuCr-oxide underlayer [5], NiAl underlayer [6] and Ar-etched Ru underlayer [7,8] has been reported to be able to decrease the grain size of the magnetic layer to below 6 nm. However, a deteriorated texture or reduction of the nucleation field of the magnetic layer was also observed. Recently, Yuan et al. reported that doping oxide into the Ru underlayer could reduce the grain size of the magnetic layer [9]. The reduction of grain size was based on a large volume fraction of oxide addition into the Ru underlayer, which deteriorated the texture of the latter. However, their report on the magnetic properties of the media with reduced grain size was insufficient for the evaluation of the effects of Ru-oxide underlayer on the recording media. A systematic understanding of the magnetic properties of the recording media with reduced grain size was important because it would be desirable to reduce grain size without deteriorating the magnetic properties for practical applications. In this paper, SiO_2 was doped into the Ru intermediate layer to reduce the grain size of the CoPt–SiO_2 magnetic layer. The effects of SiO_2 volume fraction and sputtering pressure of Ru–SiO_2 intermediate layer on the microstructure and magnetic properties of CoPt–SiO_2 magnetic recording media were studied.

2. Experiments

Granular media of CoPt–SiO_2(15 nm)/Ru–SiO_2(10 nm)/Ru_b (bottom Ru, 15 nm)/Ta (4 nm)/glass were deposited at room temperature by magnetron sputtering. The base pressure of sputtering was lower than 5×10^{-6} Pa. The Ta layer and Ru_b layer were deposited at 0.4 Pa. The Ru–SiO_2 (hereafter referred to as Ru_t) layer was deposited at 0.4 Pa and 1.3 Pa argon pressures respectively. The $Co_{72}Pt_{28}$, Ru, Ta and SiO_2 targets (made by Toshima MFG and Williams Advanced Materials with purities of 99.9%) were used for the sputtering. DC and AC sputtering were used for the metal and SiO_2 targets respectively. The volume fraction of SiO_2, adjusted by changing the sputtering time of SiO_2 relative to that of Ru, was varied from 0 to 20% in the Ru_t underlayer. The composition and thickness of the CoPt–SiO_2 layer were kept constant in all samples. Coercivities of the media were measured using

* Corresponding author. State key Laboratory of Electronic Thin Films and Integrated Devices, University of Electronic Science and Technology of China, Chengdu, 610054, China. Tel.: +86 28 83201475.
E-mail address: rjuntang@gmail.com (R. Tang).

0040-6090/$ – see front matter © 2010 Elsevier B.V. All rights reserved.
doi:10.1016/j.tsf.2010.05.083

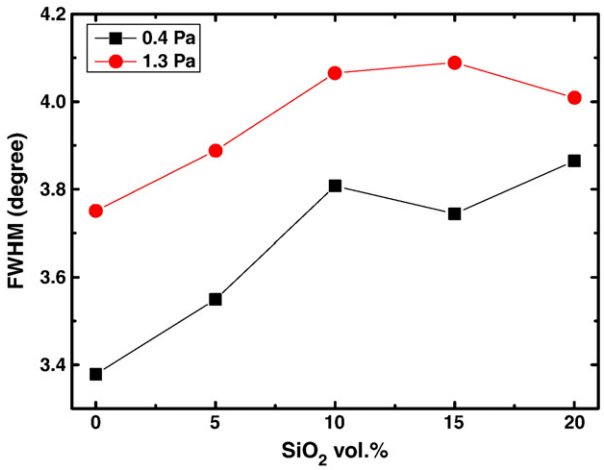

Fig. 1. The FWHM of Ru (00.2) rocking curves as a function of the SiO_2 volume fraction in the Ru_t underlayer deposited at 0.4 Pa and 1.3 Pa. The lines were only used to guide the readers' eyes.

the vibrating sample magnetometer (VSM, Lakeshore 7407) under maximum applied field of 1.2 T. Time-dependent remanent coercivities of the media were measured using the alternating gradient force magnetometer (AGFM, Princeton MicroMag 2900) under maximum applied field of 2 T. The textures of the films were investigated using Philips X'Pert X-ray diffractometer (XRD) with CuKα1 radiation (source wavelength is 1.5406 Å). The microstructures of the films were investigated using JEOL-2010 transmission electron microscope (TEM). The TEM samples of Ru_t underlayer were prepared on carbon coated Cu grids and those of CoPt–SiO_2 layers were prepared by grinding and polishing the films sputtered on glass substrates.

3. Results and discussions

Fig. 1 shows the full width at half maximum (FWHM) values of Ru (00.2) rocking curves as a function of SiO_2 volume fraction at the deposition pressures of 0.4 Pa and 1.3 Pa, respectively. For the samples deposited at 0.4 Pa, the FWHM increased from 3.4° to 3.9°. For those deposited at 1.3 Pa, the FWHM increased from 3.8° to 4.1°. The FWHM of Ru_t deposited at 0.4 Pa was smaller than those deposited at 1.3 Pa, which was attributed to the larger kinetic energy of Ru adatoms at 0.4 Pa deposition than that at 1.3 Pa deposition [10]. The texture information of the CoPt layer could not be unequivocally determined from the XRD results due to the very close lattice constant-*c* between CoPt (00.2) and Ru (00.2).

Fig. 2 shows the bright field TEM images of Ru_t layer deposited with different SiO_2 volume fractions under different pressures. Fig. 2(a) showed that for film deposited at 0.4 Pa without SiO_2 addition, the Ru grain size was very large and grain boundaries were ill defined. This was due to the high mobility of Ru adatoms at 0.4 Pa deposition. With addition of SiO_2, isolated Ru grains were observed. The grain sizes (center to center distance, averaged over randomly selected 100 pairs of grains) were 6.7 ± 0.9 nm and 5.3 ± 1.3 nm for 10% and 20% addition of SiO_2, respectively. The grain boundaries were deduced to be SiO_2 due to the phase separation between Ru and SiO_2. For films deposited at 1.3 Pa, isolated grains were observed even without SiO_2 addition as shown in Fig. 2(d). This was caused by the low mobility of Ru atoms and the "shadowing effect" [11] of Ru grains at 1.3 Pa deposition. The grain boundaries were deduced to be voids. With the addition of SiO_2, these grain boundaries became a hybrid of voids and oxides. The grain sizes were 6.6 ± 0.7 nm, 6.4 ± 0.9 nm and 4.5 ± 1.0 nm for 0%, 10% and 20% of SiO_2, respectively.

Fig. 3 shows the bright field TEM images and grain size distributions of CoPt–SiO_2 media, with Ru_t deposited at 0.4 Pa (Fig. 3(a)–(d)) and 1.3 Pa (Fig. 3(e)–(h)). The grain sizes in Fig. 3 (d) and (h) were center to center distance of two neighboring grains and counted over randomly selected 100 grain pairs. The average and standard deviations of the grain sizes, which were obtained by log-normal fitting to the data, were indicated in the figures. Addition of SiO_2 into the Ru_t layer decreased both the grain size and size distribution of CoPt grains. The reduction of grain size was attributed to the smaller Ru grains and the enhanced oxide segregation in the initial growth region of the CoPt layer [12]. The average grain size of CoPt layer with Ru_t layer deposited at 1.3 Pa was larger than that at 0.4 Pa when SiO_2 content was smaller than 20 vol.%. This is due to the better isolated Ru grains in the Ru_t layer deposited at 1.3 Pa than at 0.4 Pa, as shown in Figs. 2 and 3(c) and (g). However, although addition of SiO_2 into Ru_t layer led to smaller magnetic grain size, some of the magnetic grains became interconnected, thus increasing the exchange coupling of magnetic grains, as shown in Fig. 3(b) and (f).

Fig. 4 shows the dependence of out-of-plane hysteresis loops and coercivities of CoPt–SiO_2 media on the SiO_2 volume fraction and deposition pressure of Ru_t. For media with Ru_t deposited at 1.3 Pa, adding 5 vol.% SiO_2 into the Ru_t did not lead to noticeable changes of the coercivity. With further increase in SiO_2 content, the coercivity decreased. For media deposited at 0.4 Pa, adding SiO_2 into the Ru_t did not lead to appreciable changes of the coercivity. However, the media with Ru_t deposited at 1.3 Pa displayed higher coercivities than those with Ru_t deposited at 0.4 Pa. The coercivity of the media was determined by both the microstructure of the CoPt grains and magnetization reversal mechanism as discussed below.

In order to understand the magnetization reversal mechanism of the CoPt–SiO_2 media, angular dependent coercivities were measured. Fig. 5 shows the angular dependent coercivity curves of CoPt–SiO_2 media with Ru_t layer deposited at different pressures and with different SiO_2 volume fractions. The Stoner–Worfarth (S–W) model indicates fully exchange-decoupled magnetization reversal and domain wall motion (DWM) (Kondorsky model [13]) represents strongly exchange-coupled reversal. For films with Ru_t deposited at 0.4 Pa, adding 5 vol.% SiO_2 into the Ru_t resulted in the magnetization reversal mechanism becoming closer to the S–W mode. This is attributed to improved isolation of Ru grains and hence, better isolated CoPt grains. With a SiO_2 content of 10 vol.%, the curve did not change appreciably. With a further increase in SiO_2 content beyond 15 vol.%, the curves approached the DWM mode. When the Ru_t was deposited at 1.3 Pa, no significant changes were observed when SiO_2 content was smaller than 10 vol.%. However, the curves approached the DWM mode when SiO_2 content was larger than 10 vol.%. As seen from Fig. 1, addition of SiO_2 into the Ru_t layer deteriorated the texture of the magnetic grains, which might account for the observed changes in the curves of the angular dependent coercivities. When the SiO_2 content exceeded 10 vol.%, the sizes of Ru and CoPt grains decreased. The volume of non-magnetic grain boundary in the CoPt layer increased. As a result, the non-magnetic grain boundary in the CoPt layer would possibly be thinner if one-to-one grain growth was not realized [8]. Thinner non-magnetic grain boundary would lead to stronger exchange coupling between magnetic grains [14]. The reversal mechanisms of media with Ru_t deposited at 1.3 Pa were closer to S–W mode than those of media deposited at 0.4 Pa. This result could be attributed to the existence of void grain boundaries in the Ru_t layer deposited at 1.3 Pa which improved the grain isolation of CoPt layer as shown in Fig. 2.

Fig. 6(a) shows the activation volume (V_{act}) of the CoPt recording layer as a function of SiO_2 volume fraction in Ru_t under deposition pressures of 0.4 and 1.3 Pa. The values of V_{act} were obtained by fitting time-dependent remanent coercivities [15,16], using the least-squares method. The fitting quality was evaluated by the square of the multiple correlation coefficients R^2 where $0 \le R^2 \le 1$ with $R^2 = 1$ corresponding to perfect data fitting. R^2 of all the fittings were larger than 0.97, except for 0.4 Pa deposition with 5 vol.% SiO_2 where

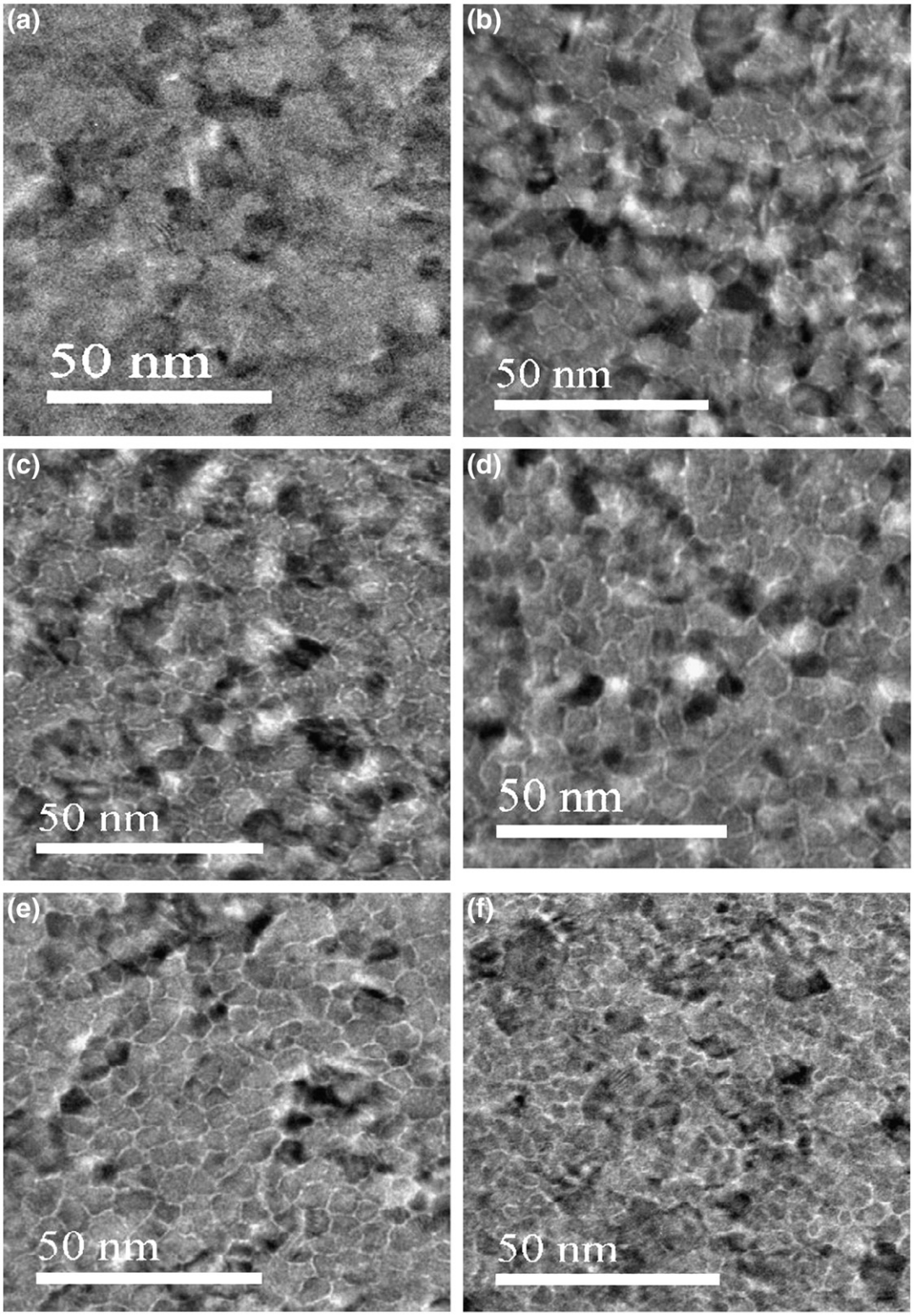

Fig. 2. Planar-view TEM images of Ru_t layer deposited with the SiO_2 volume fraction and pressure of (a) 0% and 0.4 Pa, (b) 10% and 0.4 Pa, (c) 20% and 0.4 Pa, (d) 0% and 1.3 Pa, (e) 10% and 1.3 Pa and (f) 20% and 1.3 Pa. TEM images in this figure were obtained from samples deposited on the carbon coated Cu grids.

$R^2 = 0.94$ and with 20 vol.% SiO_2 where $R^2 = 0.78$. The V_{act} was an indirect parameter of media representing the areal density [17]. The smaller the V_{act}, the higher the areal density that the media could support. For media with Ru_t deposited at 0.4 Pa, adding 5 vol.% SiO_2 into the Ru_t layer reduced V_{act} slightly. With further increase in SiO_2 beyond 5 vol.%, V_{act} increased. For media with Ru_t deposited at 1.3 Pa, adding 5 vol.% SiO_2 into the Ru_t did not result in an appreciable change in V_{act}. However, the V_{act} increased slightly with further increase in SiO_2 content. The V_{act} was determined by the size of magnetic grains and the strength of exchange coupling between these grains. Smaller grain size and weaker exchange coupling decrease the V_{act} and vice versa. For media with Ru_t deposited at 0.4 Pa, adding 5 vol.% SiO_2 into

the Ru_t led to the decrease in grain size and strength of exchange coupling between grains, since Ru_t was nearly a continuous layer without SiO_2 addition. As a result, the V_{act} decreased. However, the V_{act} of the media with Ru_t deposited at 1.3 Pa was higher than those of the media with Ru_t deposited 0.4 Pa. This was caused by the smaller and more isolated CoPt grains at 1.3 Pa compared to that at 0.4 Pa.

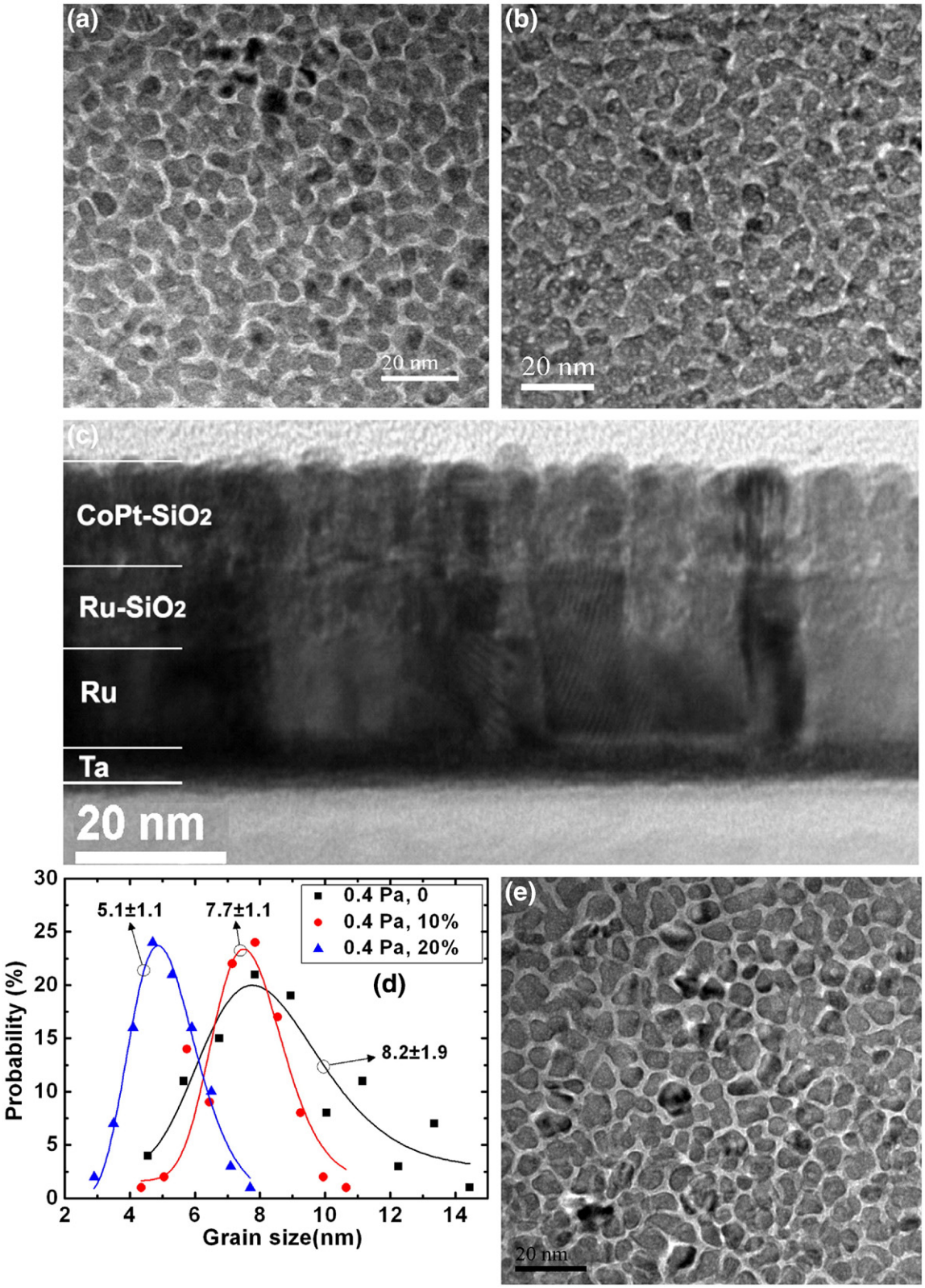

Fig. 3. A comparison of TEM images of CoPt–SiO_2 media with Ru_t deposited under different conditions. Images (a) and (b) are planar-view images deposited at 0.4 Pa without and with 10 vol.% SiO_2 in Ru_t. Images (e) and (f) are planar-view images deposited at 1.3 Pa without and with 10 vol.% SiO_2 in Ru_t. Images (c) and (g) are cross-section images of the samples in (b) and (f). Plots (d) and (h) are the grain size distributions of the CoPt media with Ru_t deposited at 0.4 Pa and 1.3 Pa and various SiO_2 additions. The TEM images were obtained from samples deposited on the glass substrates.

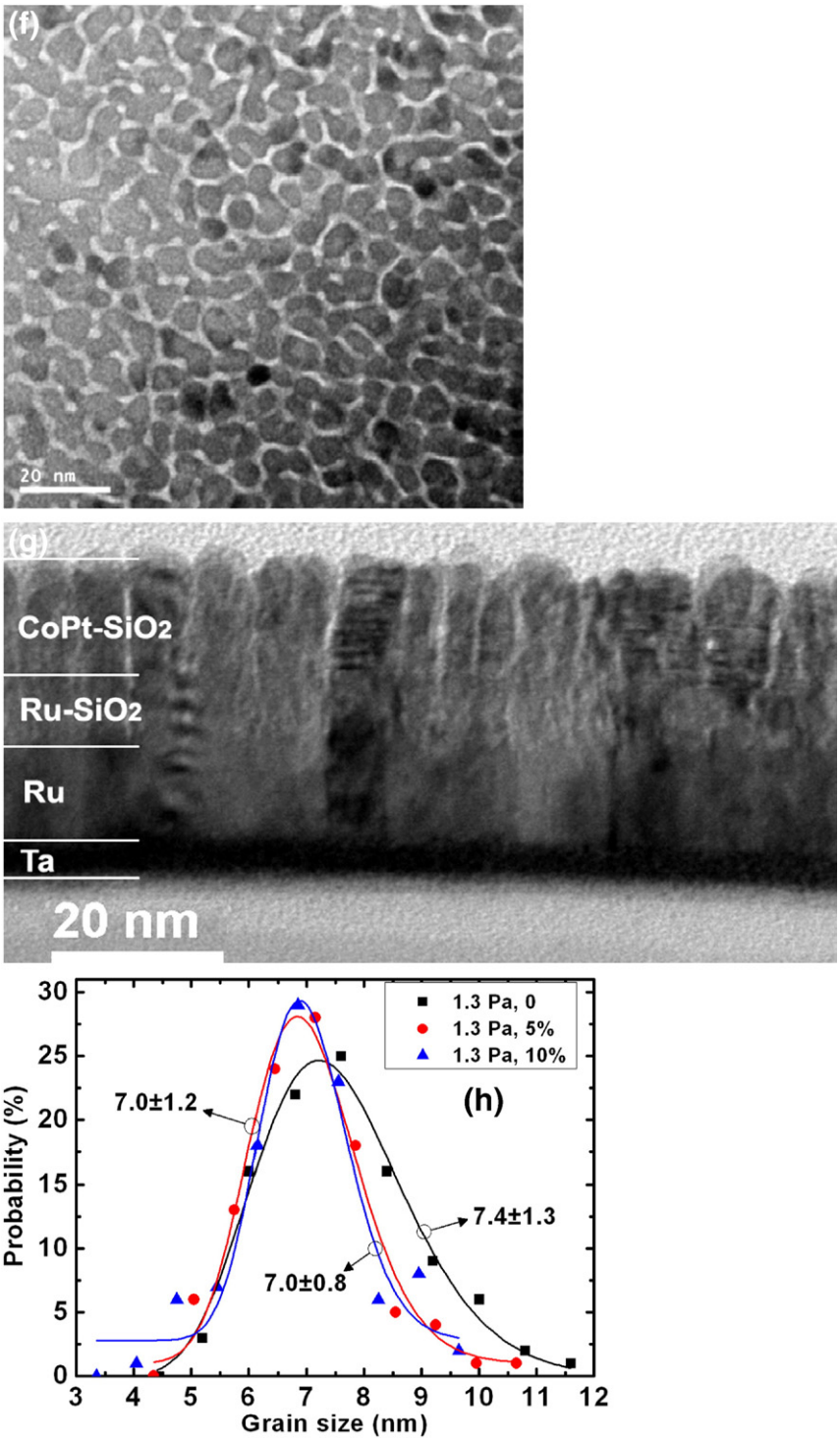

Fig. 3 (*continued*).

Fig. 6(b) and (c) shows the effective anisotropy constant (K_{ueff}) and the thermal stability factor (TSF, defined as $K_{ueff}V_{act}/k_BT$) of CoPt–SiO_2 media as a function of the SiO_2 volume fraction in Ru_t deposited at 0.4 Pa and 1.3 Pa. The TSF was obtained by fitting the time-dependent remanent coercivities into Sharrock's equation as follows [18]

$$H_c(t) = H_0\left\{1-\left[\frac{k_BT}{K_{ueff}V_{act}}\ln\frac{f_0t}{\ln 2}\right]^{\frac{1}{n}}\right\}$$

where $H_c(t)$ is the time-dependent remanent coercivity, k_B is the Boltzmann constant, T is the temperature taken as 298 K, f_0 is the attempt frequency taken as 10^9, and parameter n is taken as 2. R^2 of all the fittings were larger than 0.97, except for 0.4 Pa deposition with 5 vol.% SiO_2 where $R^2 = 0.93$ and with 20 vol.% SiO_2 where $R^2 = 0.8$. K_{ueff} was then obtained by dividing TSF by V_{act}/k_BT. For media with Ru_t deposited at 0.4 Pa, adding SiO_2 into Ru_t layer did not cause noticeable changes in K_{ueff}. However, for media with Ru_t deposited at 1.3 Pa, adding 5 vol.% SiO_2 into Ru_t layer resulted in a slight increase of K_{ueff}.

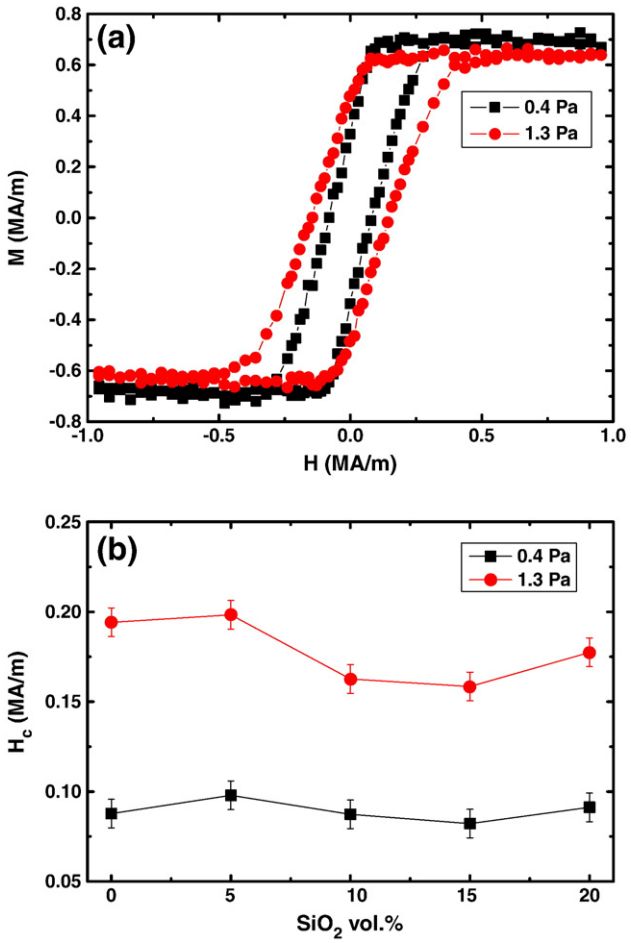

Fig. 4. Out-of-plane (a) hysteresis loops and (b) coercivities of CoPt–SiO_2 media as a function of SiO_2 volume fraction in the Ru_t deposited at 0.4 Pa and 1.3 Pa. The error bars represented the standard error of the mean. The lines were only used to guide the readers' eyes.

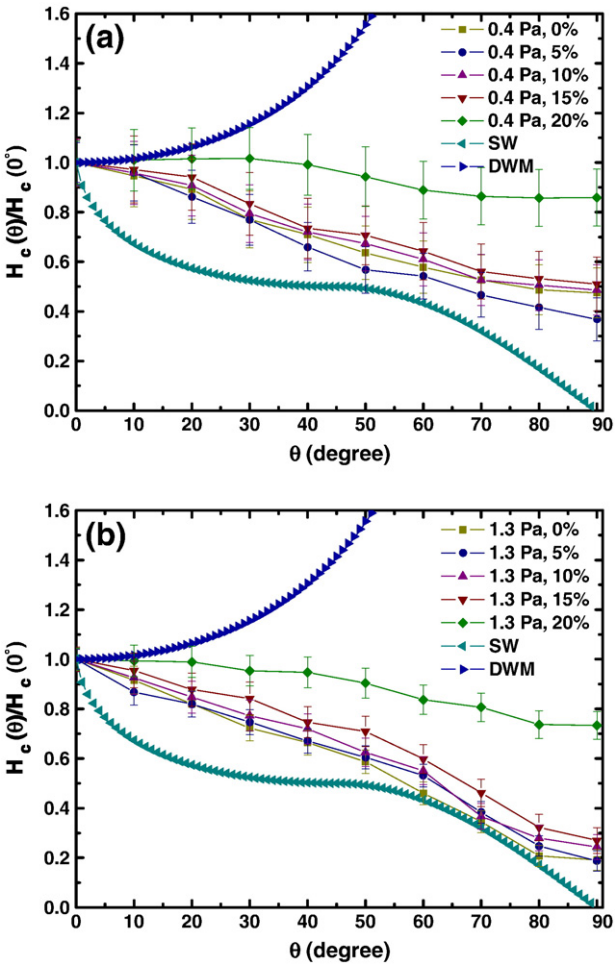

Fig. 5. Angular dependent coercivities of CoPt–SiO_2 media with Ru_t layer deposited with different SiO_2 volume fractions at (a) 0.4 Pa and (b) 1.3 Pa. The Stoner–Worfarth (S–W) model and domain wall motion (DMW) model are plotted as references. The error bars represented the standard error of the mean. The widths of the error bars were estimated from the step size of applied field around the coercivities (16 kA/m). The lines were only used to guide the readers' eyes.

The K_{ueff} decreased when SiO_2 content was 10 vol.%. Further increasing SiO_2 content did not change K_{ueff} appreciably. From Fig. 6(c), for media with Ru_t deposited at 0.4 Pa, adding 5 vol.% SiO_2 into Ru_t layer decreased the TSF slightly. Further increasing SiO_2 content beyond 5 vol.% resulted in a slight increase in TSF. When Ru_t was deposited at 1.3 Pa, adding 5 vol.% SiO_2 into the Ru_t layer increased the TSF. When SiO_2 was increased to 10 vol.%, the TSF decreased. Further increasing SiO_2 content beyond 10 vol.% did not change TSF appreciably. The TSF is proportional to the product of K_{ueff}, which is determined by the microstructure of the film [19], and V_{act} (which is determined by the grain size and exchange decoupling between the grains). Therefore, the changes of microstructure, grain size and exchange coupling affected the TSF.

4. Summary

In this paper, the effects of SiO_2 volume fraction and sputtering pressure of Ru_t layers on the microstructure of the layers and the magnetic properties of CoPt–SiO_2 recording media were studied. When Ru_t layer was deposited at 0.4 Pa, the sizes of the Ru and CoPt grains decreased from 6.7 ± 0.9 to 5.3 ± 1.3 and from 8.2 ± 1.9 to 5.1 ± 1.1 with the addition of SiO_2 up to 20 vol.% respectively, but their *c*-axis orientations slightly deteriorated. Increasing the deposition pressure of the Ru_t layer from 0.4 Pa to 1.3 Pa further reduced the grain size due to the porosity in the grain boundary regions of the Ru_t layer. Addition of 5 vol.% SiO_2 into the Ru_t layer increased the coercivity, the exchange decoupling and the thermal stability of the CoPt layer. However, further increase of SiO_2 volume fraction in the Ru_t layer decreased the grain size, the coercivity and the exchange decoupling, degrading the thermal stability of the CoPt layer. On the other hand, CoPt media with Ru_t layer deposited at 1.3 Pa showed a much higher coercivity, better exchange decoupling and better thermal stability than those of the media with Ru_t layer deposited at 0.4 Pa. The above results suggest that small amounts of SiO_2 addition and deposition pressure of 1.3 Pa can reduce the grain size of the Ru_t layer and hence, the recording layer without adversely affecting the magnetic properties of the recording layer.

Acknowledgements

The authors thank the technical support from Prof. Chow Gan-Moog and Assistant Prof. Dr. Chen Jingsheng, as well as helpful discussions with Dr. Pandey Koashal Kishor Mani from the National University of Singapore (NUS) and Dr. Hu Jiangfeng from the Data Storage Institute in Singapore. The author R.J. Tang thanks the support of Scholarship from the China Scholarship Council. This work is partially supported by the Agency for Science, Technology and Research (A*STAR) Singapore under Grant No. 062-101-0021, and FRC of NUS under Grant No. R-284-000-053-112.

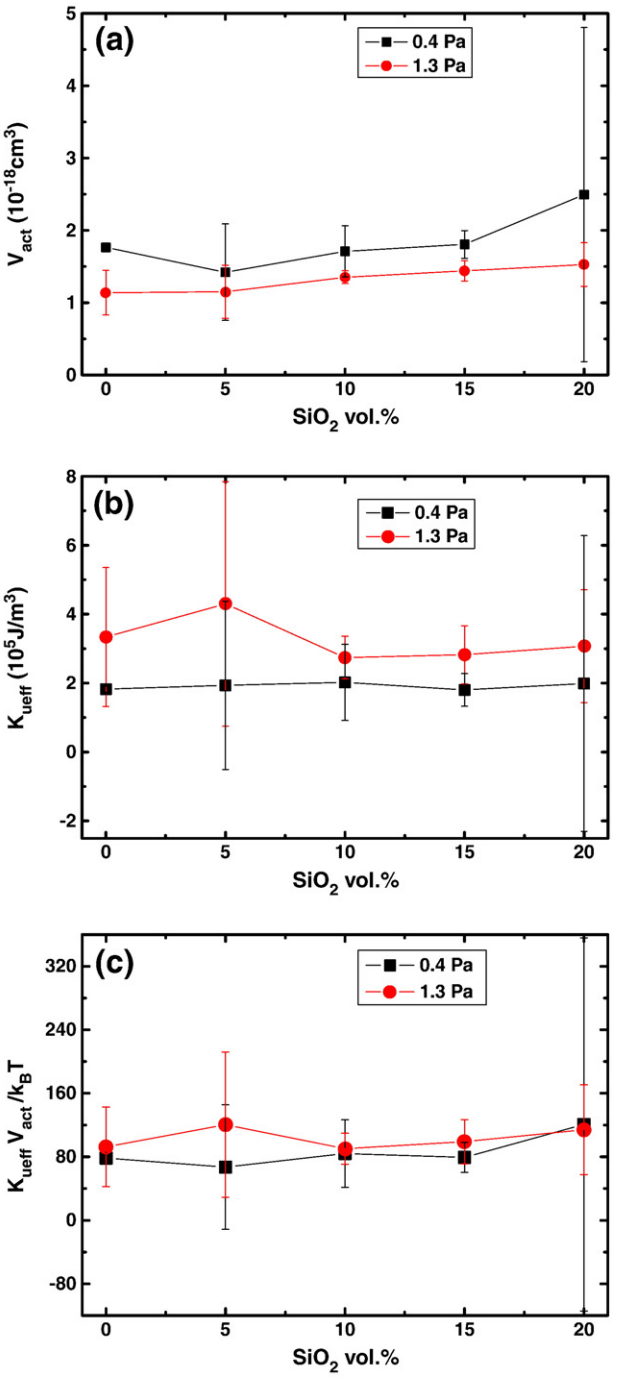

Fig. 6. Plot (a) activation volume (V_{act}), (b) effective anisotropy constant (K_{ueff}) and (c) thermal stability factor of the CoPt–SiO_2 recording media as a function of the SiO_2 volume fraction in Ru_t deposited at 0.4 Pa and 1.3 Pa. The error bars represented the 95% confidence interval on the estimates of the paramaters obtained by fit. The lines were only used to guide the readers' eyes.

References

[1] S. Iwasaki, IEEE Trans. Magn. MAG-20 (1984) 657.
[2] M. Zheng, B.R. Acharya, G. Choe, J.N. Zhou, Z.D. Yang, E.N. Abarra, K.E. Johnson, IEEE Trans. Magn. 40 (2004) 2498.
[3] Y. Inaba, T. Shimatsu, T. Oikawa, H. Sato, H. Aoi, H. Muraoka, Y. Nakamura, IEEE Trans. Magn. 40 (2004) 2486.
[4] S.N. Piramanayagam, C.K. Pock, L. Li, C.Y. Ong, C.S. Mah, J.Z. Shi, Appl. Phys. Lett. 89 (2006) 162504.
[5] S.N. Piramanayagam, J.Z. Shi, H.B. Zhao, C.K. Pock, C.S. Mah, C.Y. Ong, J.M. Zhao, J. Zhang, Y.S. Kay, L. Lu, IEEE Trans. Magn. 43 (2007) 633.
[6] H. Yuan, Y.L. Qin, D.E. Laughlin, Thin Solid Films 517 (2008) 990.
[7] H. Yuan, D.E. Laughlin, Appl. Phys. Lett. 93 (2008) 102511.
[8] H. Yuan, D.E. Laughlin, J. Appl. Phys. 105 (2009) 07B707.
[9] H. Yuan, D.E. Laughlin, X. Zhu, B. Lu, J. Appl. Phys. 103 (2008) 07F513.
[10] K.K.M. Pandey, J.S. Chen, B.C. Lim, G.M. Chow, J. Appl. Phys. 104 (2008) 073904.
[11] J.A. Thornton, J. Vac. Sci. Technol. A. 4 (1986) 3095.
[12] I. Takekuma, R. Araki, M. Igarashi, H. Nemoto, I. Tamai, Y. Hirayama, Y. Hosoe, J. Appl. Phys. 99 (2006) 08E713.
[13] E. Kondorsky, J. Phys. (Moscow) II (1940) 161.
[14] V. Sokalski, D.E. Laughlin, J.-G. Zhu, Appl. Phys. Lett. 95 (2009) 102507.
[15] Z.S. Shan, Y.F. Xu, J.P. Wang, T.C. Chong, S.S. Malhotra, D.C. Staffort, C.X. Zhu, IEEE Trans. Magn. 37 (2001) 1944.
[16] Y. Inaba, T. Shimatsu, H. Muraoka, J.D. Dutson, K. O'Grady, IEEE Trans. Magn. 41 (2005) 3130.
[17] S.M. Stinnett, J.W. Harrell, A.F. Khapikov, W.D. Doyle, IEEE Trans. Magn. 36 (2000) 148.
[18] M.P. Sharrock, J. Appl. Phys. 76 (1994) 6413.
[19] T. Shimatsu, Y. Okazaki, H. Sato, O. Kitakami, S. Okamoto, H. Aoi, H. Muraoka, Y. Nakamura, IEEE Trans. Magn. 43 (2007) 2995.